Identification of Time-Varying Intrinsic and Reflex Joint Stiffness

Daniel Ludvig*, *Member, IEEE*, Tanya Starret Visser, Heidi Giesbrecht, and Robert E. Kearney, *Fellow, IEEE*

***Abstract*—Dynamic joint stiffness defines the dynamic relationship between the position of a joint and the torque acting about it and can be separated into intrinsic and reflex components. Under stationary conditions, these can be identified using a nonlinear parallel-cascade algorithm that models intrinsic stiffness—a linear dynamic response to position—and reflex stiffness—a nonlinear dynamic response to velocity—as parallel pathways. Experiments using this method show that both intrinsic and reflex stiffness depend strongly on the operating point, defined by position and torque, likely because of some underlying nonlinear behavior not modeled by the parallel-cascade structure. Consequently, both intrinsic and reflex stiffness will appear to be time-varying whenever the operating point changes rapidly, as during movement. This paper describes and validates an extension of the parallel-cascade algorithm to time-varying conditions. It describes the ensemble method used to estimate time-varying intrinsic and reflex stiffness. Simulation results demonstrate that the algorithm can track rapid changes in joint stiffness accurately. Finally, the performance of the algorithm in the presence of noise is tested. We conclude that the new algorithm is a powerful new tool for the study of joint stiffness during functional tasks.**

***Index Terms*—Biological system modeling, joint stiffness, time-varying (TV) systems.**

I. Introduction

DYNAMIC joint stiffness is an important property of the peripheral neuromuscular system that quantifies the dynamic relationship between the position of a joint and the torque acting about it [1]. Joint stiffness may be separated into two components: intrinsic stiffness, encompassing the mechanical properties of the joint, active muscle, and passive visco-elastic tissues; and reflex stiffness, arising from changes in muscle activation due to the stretch reflex.

How the central nervous system (CNS) modulates stiffness and the role of intrinsic and reflex mechanisms during the execution of a movement remains a topic of debate [2]–[5]. Studies under stationary conditions show that joint stiffness is highly dependent on joint position and torque [6]; this will result in large changes in intrinsic and reflex stiffness during movement. However, these changes are difficult to characterize because they occur together, are rapid, and depend strongly on the phase, amplitude, and speed of the motion [7], [8]. Reflexes are particularly elusive, because their nonlinear behavior and tight coupling to intrinsic effects make it difficult to determine their functional role [9], despite the apparent simplicity of the monosynaptic pathway connecting muscle spindle afferents to motor neurons [9], [10].

Many studies have evaluated reflexes in terms of electromyograph (EMG) responses [7], [8], [11], [12] and found that they are modulated substantially during various tasks and movements. Kearney *et al.* [7] examined the stretch reflex response during an imposed gait movement and found that reflex EMG responses were significantly lower during movement than at matched stationary positions throughout the walking cycle. Kirsch *et al.* [13] imposed a rapid ramp movement at the ankle joint while subjects maintained various levels of tonic muscle activation. Their results suggested that the stretch reflex was modulated independently of motor neuron pool activation level and that this behavior was mediated largely by peripheral mechanisms.

A major problem in determining the functional role of stretch reflexes is that it is difficult to distinguish torques arising from reflex activity from those due to intrinsic properties of the joint and muscles [14]. Reflex EMG alone does not define the mechanical effects of reflexes since muscle dynamics, characterized by nonlinear force–length and force–velocity relations, are a key factor in force generation [7]. Therefore, simultaneous analysis of intrinsic and reflex mechanisms is required to understand the functional role of the stretch reflex.

Previously, our laboratory developed a parallel-cascade (PC) nonlinear system identification method to separate intrinsic and reflex contributions to dynamic joint stiffness under stationary conditions [14]. This PC algorithm models the dynamic relation between joint position and torque with separate pathways for intrinsic and reflex mechanisms. The method uses time-invariant (TI) techniques to evaluate intrinsic and reflex properties at a specific operating point, such as a particular posture or contraction level. The technique has been used successfully to estimate joint dynamics for a variety of operating conditions in both normal subjects as well as in patients with spasticity resulting from spinal cord injuries and stroke [6], [15], [16].

The results of these studies demonstrate that the nonlinear PC model describes intrinsic and reflex stiffness well for small perturbations about a fixed operating point. However, the PC

Manuscript received October 5, 2010; accepted January 8, 2011. Date of publication February 10, 2011; date of current version May 18, 2011. This work was supported in part by the Natural Sciences and Engineering Research Council of Canada (NSERC) and in part by the Canadian Institutes of Health Research (CIHR). *Asterisk indicates corresponding author.*

*D. Ludvig was with the Biomedical Engineering Department, McGill University, Montreal, QC H3 A 2B4, Canada. He is now with the Sensory Motor Performance Program, Rehabilitation Institute of Chicago, Chicago, IL 60657 USA (e-mail: daniel.ludvig@mail.mcgill.ca).

T. S. Visser, H. Giesbrecht, and R. E. Kearney are with the Biomedical Engineering Department, McGill University, Montreal, QC H3 A 2B4, Canada (e-mail: tanya.starret@mail.mcgill.ca; heidi.giesbrecht@mail.mcgill.ca; robert.kearney@mcgill.ca).

Color versions of one or more of the figures in this paper are available online at http://ieeexplore.ieee.org.

Digital Object Identifier 10.1109/TBME.2011.2113184

0018-9294/$26.00 © 2011 IEEE

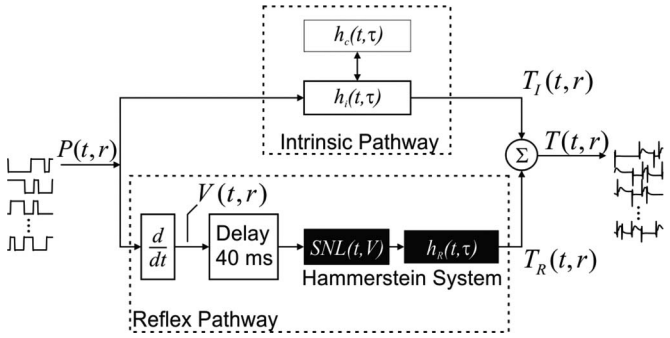

Fig. 1. Block diagram of the TVPC model of ankle stiffness. Position and torque are functions of time t and realization r; IRFs are functions of time t and lag τ; the static nonlinearity is a function of time t and joint velocity V.

algorithm cannot estimate joint stiffness under time-varying (TV) conditions. Thus, the time course of stiffness changes when the joint moves from one operating point to another remains unknown. This information is required to understand the role of reflexes in the initiation and control of movement. Ludvig and Kearney [17] tracked the changes in joint stiffness while subjects altered the background torque level. However, their algorithm responded sluggishly to changes in joint stiffness and, thus, could not measure quick changes in stiffness accurately. This was due to the time needed for averaging, and thus, any similar adaptive algorithm will also suffer from the limitation of not being able to measure quick changes in joint stiffness.

This paper describes and validates the extension of the PC method to TV conditions. The new algorithm employs ensemble methods and PC methods to estimate TV intrinsic and reflex stiffness [14], [18], [19]. This time-varying parallel-cascade (TVPC) algorithm estimates intrinsic and reflex stiffness at each sample time allowing changes in intrinsic and reflex dynamics to be tracked throughout movements.

This paper is developed as follows: Section II describes the TVPC algorithm, details the iterative procedure, and shows how ensemble methods are integrated into the PC structure for identification of TV intrinsic and reflex dynamics. Section III examines the performance limits of the algorithm using simulated data. Section IV discusses the results with specific attention to the adequacy of the TVPC model. Some of these results have been the subject of conference presentations [20]–[22].

II. Identification Algorithm

Fig. 1 shows the TVPC model for joint stiffness. The upper intrinsic pathway relates joint position to torque via a TV linear dynamic element. The lower reflex pathway relates joint position to torque via a differentiator and a TV Hammerstein system, comprising a static nonlinear element in series with a linear dynamic element [23]. The contributions from the two pathways are assumed to add linearly to give the total torque about the joint.

As in the TI case, the output at any time can be predicted by convolving the input with an impulse response function (IRF). However, in contrast to the TI case, in the TV case the IRF changes with each time point so that the discrete TV convolution can be expressed as

$$y(i) = \sum_{j=M1}^{M2} h(i,j)\, u(i-j) \tag{1}$$

where $y(i)$ is the output at sample time i, $u(i-j)$ is the input at sample time $i-j$, and $h(i,j)$ is the IRF at time i and lag j.

Identification of the TV model is achieved using an iterative algorithm where the two pathways are identified sequentially using ensemble techniques. This requires an ensemble of position input records $P(t,r)$ and torque output records $T(t,r)$ that are functions of time t and realization number r as Fig. 1 illustrates. It will be assumed that: 1) the input realizations are uncorrelated with each other; and 2) the system varies with time in the same way for all realizations.

Section II-A will describe the estimation of the TV intrinsic pathway. Section II-B will describe the estimation of the TV reflex stiffness. Section II-C will describe how the two methods are combined.

A. Estimation of TV Intrinsic Stiffness

Intrinsic stiffness is estimated by computing a linear TV IRF between the position and the intrinsic torque. A detailed explanation of the method used to compute the linear TV IRF is presented in [18], and will only be summarized briefly here.

A linear TV IRF can be found by computing the relationship between the TV input-output cross correlation and the time TV input autocorrelation. The difference between TI correlation functions and TV correlation functions is that for the TI functions the estimates are independent of sample time and the averaging is performed along the entire signal length. In the TV case, correlation functions are estimated at each time point and the averaging is performed across realizations.

The discrete TV correlation between the intrinsic torque T_I at sample time i and the position at sample time $i-k$ is

$$\hat{\phi}_{\mathrm{TP}}(i,-k) = \frac{1}{R}\sum_{r=1}^{R} T_I(i,r)\, P(i-k,r) \tag{2}$$

where r is the realization number and R is the total number of realizations. Similarly, the discrete TV correlation between the position at sample times $i-j$ and $i-k$ is

$$\hat{\phi}_{\mathrm{PP}}(i-k,k-j) = \frac{1}{R}\sum_{r=1}^{R} P(i-j,r)\, P(i-k,r). \tag{3}$$

The relationship between the TV position-intrinsic torque cross correlation and the TV position autocorrelation is

$$\hat{\phi}_{\mathrm{TP}}(i,-k) = \Delta t \sum_{j=M1}^{M2} h_I(i,j)\hat{\phi}_{\mathrm{PP}}(i-k,k-j) \tag{4}$$

where h_I is the TV intrinsic stiffness IRF, and $M1$ and $M2$ are the minimum and maximum lags over which the IRF is computed. Letting k take values from $M1$ to $M2$, (4) can be written in matrix form as

$$\hat{\mathbf{\Phi}}_{\mathbf{TP}}(i) = \Delta t \hat{\mathbf{\Phi}}_{\mathbf{PP}}\mathbf{h_I}(i) \tag{5}$$

where, $\hat{\mathbf{\Phi}}_{\mathbf{PP}}(i)$ and $\hat{\mathbf{\Phi}}_{\mathbf{TP}}(i)$ are shown at the bottom of this page and

$$\mathbf{h_I}(i) = \left[h_I(i, M1) \cdots h_I(i,0) \cdots h_I(i, M2) \right]^{\mathrm{T}}.$$

In the presence of output noise, solving (5) directly leads to large random errors; instead a pseudoinverse approach is taken. Details of the pseudoinverse approach can be found in [18].

B. Estimation of TV Reflex Stiffness

Reflex stiffness is estimated by finding a TV Hammerstein system between the velocity *V* and the reflex torque. A Hammerstein system consists of a static nonlinearity followed in series by a dynamic linear element (see Fig. 1). In a TV Hammerstein system, both the static nonlinearity and the dynamic linear element vary with time. TV identification of Hammerstein system is presented in detail in [19] and will only be briefly discussed here.

Hammerstein system identification works by iteratively fixing one component—either the static nonlinearity or the dynamic linear element—and estimating the other. Once the predicted output of the estimated Hammerstein system fails to account for more of the output variance, the iteration ceases.

The initial estimate of the dynamic linear element is computed as in (5), except the input is velocity and the output is reflex torque. In the first step of the iterative component of the algorithm, the dynamic linear element is fixed and the static nonlinearity is estimated. The static nonlinearity is estimated by minimizing the difference between the predicted reflex torque $\hat{T}_R$ and the actual reflex torque T_R. The reflex torque for each realization can be predicted by convolving the output of the static nonlinearity with the reflex stiffness IRF h_R. This can be written in matrix form as

$$\mathbf{T_R}(i) = \mathbf{A}(i)\,\mathbf{p}(i) + \mathbf{e} \tag{6}$$

where $\mathbf{A}(i)$ and $\mathbf{T_R}(i)$ are shown at the bottom of this page and

$$\mathbf{p}(i) = \left[p_0(i)\ p_1(i) \cdots p_N(i) \right]^{\mathrm{T}}$$

where p_N are the *n*th-order coefficients of the static nonlinearity. The minimization of the difference between predicted and actual outputs is done by solving (6) using least squares.

A similar procedure is carried out to estimate the dynamic linear elements. The following equation is solved using least squares to estimate the dynamic linear element:

$$\mathbf{T_R}(i) = \Delta t \mathbf{B}(i)\,\mathbf{h_R}(i) + \mathbf{e} \tag{7}$$

where

$$\mathbf{B}(i) = \begin{bmatrix} \sum_{n=0}^{N} p_n(i)\,V(i - M1, 1)^n & \cdots & \sum_{n=0}^{N} p_n(i)\,V(i - M2, 1)^n \\ \vdots & \ddots & \vdots \\ \sum_{n=0}^{N} p_n(i)\,V(i - M1, R)^n & \cdots & \sum_{n=0}^{N} p_n(i)\,V(i - M2, R)^n \end{bmatrix}$$

$$\mathbf{h_R}(i) = \left[h_R(i, M1) \cdots h_R(i, M2) \right]^{\mathrm{T}}$$

and $\mathbf{T_R}$ is the same as in (6).

The two least-squares computations are iterated until the sum of squared differences between the actual and predicted output fails to increase.

C. Concurrent Estimation of Intrinsic and Reflex Stiffness

In Sections II-A and II-B, we have described algorithms to estimate TV linear and Hammerstein systems. Estimating intrinsic and reflex stiffness would be simple if we could just measure the intrinsic and reflex torques and apply the equations presented

$$\hat{\mathbf{\Phi}}_{\mathbf{PP}}(i) = \begin{bmatrix} \hat{\phi}_{\mathrm{PP}}(i - M1, 0) & \hat{\phi}_{\mathrm{PP}}(i - M1, -1) & \cdots & \hat{\phi}_{\mathrm{PP}}(i - M1, M1 - M2) \\ \hat{\phi}_{\mathrm{PP}}(i - M1 - 1, 1) & \hat{\phi}_{\mathrm{PP}}(i - M1 - 1, 0) & \cdots & \hat{\phi}_{\mathrm{PP}}(i - M1 - 1, M1 - M2 + 1) \\ \vdots & \vdots & \ddots & \vdots \\ \hat{\phi}_{\mathrm{PP}}(i - M2, M2 - M1) & \hat{\phi}_{\mathrm{PP}}(i - M2, M2 - M1, 1) & \cdots & \hat{\phi}_{\mathrm{PP}}(i - M2, 0) \end{bmatrix}$$

$$\hat{\mathbf{\Phi}}_{\mathbf{TP}}(i) = \left[\hat{\phi}_{\mathrm{TP}}(i, -M1) \quad \hat{\phi}_{\mathrm{TP}}(i, -M1 - 1) \quad \cdots \hat{\phi}_{\mathrm{TP}}(i, -M2) \right]^{T}$$

$$\mathbf{A}(i) = \begin{bmatrix} \Delta t \sum_{j=M1}^{M2} h_R(i,j) & \Delta t \sum_{j=M1}^{M2} h_R(i,j)\,V(i-j,1) & \cdots & \Delta t \sum_{j=M1}^{M2} h_R(i,j) V(i-j,1)^N \\ \Delta t \sum_{j=M1}^{M2} h_R(i,j) & \Delta t \sum_{j=M1}^{M2} h_R(i,j)\,V(i-j,2) & \cdots & \Delta t \sum_{j=M1}^{M2} h_R(i,j)\,V(i-j,2)^N \\ \vdots & \vdots & \ddots & \vdots \\ \Delta t \sum_{j=M1}^{M2} h_R(i,j) & \Delta t \sum_{j=M1}^{M2} h_R(i,j)\,V(i-j,R) & \cdots & \Delta t \sum_{j=M1}^{M2} h_R(i,j)\,V(i-j,R)^N \end{bmatrix}$$

$$\mathbf{T_R}(i) = \left[T_R(i,1)\ T_R(i,2) \cdots T_R(i,R) \right]^{\mathrm{T}}$$

in the previous two sections. However, measuring intrinsic and reflex torques is not possible; thus, a method is needed to separate the two torques. Kearney *et al*. [14] took advantage of the delay in the reflex pathway and designed an iterative algorithm (the PC algorithm) to separate the two torques. Combining the TV methods presented in the previous sections with the PC algorithm gives the TVPC algorithm, which works as follows.

1) Intrinsic stiffness is estimated using the method described in Section II-A, however, using the net torque rather than intrinsic torque. By limiting the length of the IRF to less than the reflex delay, reflex torque will simply act as uncorrelated noise.
2) $\hat{h}_I(t,\tau)$ is convolved with the position ensemble to predict the intrinsic torque $\hat{T}_I(t,r)$ that is used to estimate the intrinsic residual torque

$$\hat{T}_{\mathrm{IR}}(t,r) = T(t,r) - \hat{T}_I(t,r). \tag{8}$$

3) The static nonlinear element $\hat{\mathrm{SNL}}(t,V)$ and linear TV impulse response functions $\hat{h}_R(t,\tau)$ of the reflex pathway are estimated using the ensemble Hammerstein method described in Section II-B, treating velocity as the input and $\hat{T}_{\mathrm{IR}}(t,r)$ as the output. The reflex delay is incorporated into $\hat{h}_R(t,\tau)$ and $\hat{\mathrm{SNL}}(t,V)$ is approximated by a polynomial.
4) The reflex torque $\hat{T}_R(t,r)$ is estimated by transforming the differentiated position input ensemble with $\hat{\mathrm{SNL}}(t,V)$ and convolving it with $\hat{h}_R(t,\tau)$. The reflex residual torque is computed as

$$\hat{T}_{\mathrm{RR}}(t,r) = T(t,r) - \hat{T}_R(t,r). \tag{9}$$

5) The total predicted torque is computed as

$$\hat{T}(t,r) = \hat{T}_I(t,r) + \hat{T}_R(t,r). \tag{10}$$

6) The quality of the identification is evaluated in terms of the percent variance accounted for (%VAF) between the observed X and predicted $\hat{X}$ total torque ensembles

$$\%\mathrm{VAF}(X,\hat{X}) = 100\left(1 - \frac{\mathrm{var}(X-\hat{X}}{\mathrm{var}\,(X)}\right). \tag{11}$$

7) The procedure is repeated from step 1, using $\hat{T}_{\mathrm{RR}}(t,r)$ as the output for the identification of intrinsic stiffness. The procedure continues until the %VAF fails to increase.

Following the identification, intrinsic stiffness is converted to intrinsic compliance $h_C(t,\tau)$ because it is more readily interpreted and is less susceptible to high-frequency noise.

The TVPC algorithm distributes the overall gain of the reflex pathway arbitrarily between the nonlinear and linear elements. To standardize this, a straight line was fit to the positive half of the nonlinearity and its slope used as an estimate of the gain of the nonlinearity. The IRF and the nonlinearity were then scaled to assign all the gain to the IRF.

III. Simulation Study

We used simulated data to confirm that the algorithm could identify TV intrinsic and reflex stiffness accurately and to explore key factors influencing its performance.

A. Methods

A TV model of ankle stiffness was simulated using Simulink (The Mathworks, Inc.). Intrinsic stiffness was modeled as a second-order system

$$\mathrm{TQ}\,(t) = \mathrm{I}\ddot{\mathrm{P}} + B\,(t)\,\dot{P} + K\,(t)\,P \tag{12}$$

where K, B, and I are the elastic, viscous, and inertial parameters, respectively.

Reflex stiffness was modeled as a differentiator in series with a 40-ms delay, followed by a Hammerstein system, consisting of a half-wave rectifier in series with a second-order low-pass filter with gain $G(t)$, damping ζ, and natural frequency ω.

Theoretically, all parameters could be TV but only K, B, and G were varied with time in this study, because previous studies showed that these are the parameters that vary the most with changes in operating point [6], [24], [25]. Gaussian white noise was added to the output to simulate measurement noise; its amplitude was adjusted to generate the desired SNR. The input signal, which was similar to that used in experiments, consisted of a 0.03-rad pseudorandom binary sequence with a 150-ms switching rate, and filtered by a second-order Butterworth filter with a 50-Hz cut-off to represent the low-pass properties of our ankle actuator.

Input-output ensembles were generated by simulating the model repeatedly with the same parameters but with different realizations of input and noise sequences. Simulations were run using a fixed 1-kHz sampling rate; data were decimated to 200 Hz prior to inputting into the TVPC system identification algorithm. The intrinsic compliance and reflex stiffness IRFs were parameterized by fitting them to second-order low-pass filters using the Levenberg–Marquardt nonlinear least-squares algorithm [26].

Under some conditions, such as very low SNRs, the TVPC algorithm failed at the first iteration, and consequently, the resulting model accounted for none of the observed torques. For such cases, the %VAF was set to zero.

The results of the TVPC algorithm were compared to those from an adaptive intrinsic and reflex stiffness estimation algorithm [17]. This adaptive algorithm requires an input signal with special properties; consequently, the data for this comparison were generated by repeating the simulation with the special input signal.

For clarity, we will use the following terms: a *realization* or *trial* will refer to an individual simulation run; a *set* will refer to an ensemble of realizations with the same parameter values; a *series* will refer to a collection of sets, having different parameter values used to investigate a property of interest. Table I summarizes the parameter values used in each simulation series.

TABLE I
SIMULATION PARAMETER VALUES

Series	1	2	3	4
K (Nm/rad)	Fig. 2A	50 to 150	150	150
B (Nm/rad/s)	Fig. 2B	1.5	1.5	1.5
I (Nm/rad/s^2)	0.02	0.02	0.02	0.02
G (Nm/rad/s)	Fig. 2C	5 to 15	Fig. 5A	Fig. 5A
ζ	0.75	0.75	0.75	0.75
ω (rad/s)	20	20	20	20
SNR (dB)	∞	∞	Fig. 5C	Fig. 5C
Realizations	600	600	1000	200 to 1000, in increments of 50

B. Results

1) Rapid Changes in System Dynamics: The first simulation series assessed the TVPC algorithm's ability to track rapid changes in system dynamics. To accomplish this, K, B, and G were varied with the time courses shown in Fig. 3(a)–(c).

G underwent three step changes, whereas K and B were varied with ramp waveforms. The time courses of these changes were not designed to resemble any physiological modulation pattern since these remain unknown. Rather they were chosen to test the algorithm's ability to track rapid changes in dynamics and to determine whether the resulting parameter estimates were independent. The top row of Fig. 2 shows how these changes affected the simulated ensembles of intrinsic compliance IRFs, reflex nonlinearities, and reflex stiffness IRFs. These were obtained by computing the theoretical impulse responses of the intrinsic compliance and the reflex stiffness at each time point. The increases in the intrinsic compliance IRFs, associated with the changes in K and B, are evident in Fig. 2(a) at about 4 and 6 s, respectively. Similarly, the step changes in the reflex gain are evident in the abrupt changes in the reflex IRFs amplitudes, shown in Fig. 2(c). The static nonlinearity remains unchanged.

The bottom row of Fig. 2 shows the nonparametric system estimates produced by the TVPC algorithm. These were very similar to those simulated. Thus, the ensemble of intrinsic compliance estimates [see Fig. 2(d)] closely resembled those simulated [see Fig. 2(a)]; the peaks due to the ramp changes in K and B are clearly visible. Similarly, the reflex stiffness IRFs [see Fig. 2(f)] closely resemble the simulated values and the step changes in G are evident. The polynomial estimates of the nonlinearity [see Fig. 2(e)] resemble the simulated half-wave rectifier [see Fig. 2(b)]. Importantly, changes in simulated values of the intrinsic parameters had no effect on the estimated reflex dynamics nor did changes in the reflex parameters influence the intrinsic dynamics.

In addition, the stiffness estimates predicted the simulated torques very accurately. Thus, the ensemble %VAFs, between the simulated and predicted torques, were 98.5% for the total, 98.3% for the intrinsic, and 96.8% for the reflex torques.

Furthermore, the values for K, B, and G estimated by fitting the IRFs to parametric models to the IRFs behaved as expected. These parameter estimates, shown in the right column of Fig. 3, closely followed the simulated values, shown in the left column. Indeed, even step changes in G were tracked instantaneously. In addition, changes in any one parameter had little effect on the other parameter estimates.

We noted that the values estimated for B were slightly higher than the true values. We believe that this was related to the sampling rate used for the identification, since increasing the sampling rate eliminated this bias error at the cost of greatly increased random error.

2) Comparison to Adaptive Algorithm: The objective of the second series was to compare the TVPC algorithm to an adaptive algorithm. Fig. 4 compares the estimates generated by the TVPC algorithm to those generated by the adaptive algorithm while K and G underwent step changes. The TVPC algorithm responded to the changes in K and G instantly, while the adaptive algorithm required approximately 10 s to produce correct estimates. Furthermore, unlike the TVPC algorithm, changes in one parameter biased the adaptive algorithm estimates of the other parameter.

3) SNR: The objective of the third simulation series was to evaluate the algorithm's performance in the presence of noise and explore how this varied with the relative strength of the intrinsic and reflex pathway.

The series comprised of 1000 realizations where SNR and reflex gain both varied with time. The reflex gain was varied periodically with time as shown in Fig. 5(a) to evaluate the effect of changing the relative contributions of intrinsic and reflex mechanisms. The reflex gain varied from a low value where the reflex pathway accounted for only 15% of the net torque to a high value where it accounted for 50%. The variance of the noise [see Fig. 5(b)] increased linearly with time so that the SNR [see Fig. 5(c)] decreased from 30 to 0 dB over the run. This behavior made it possible to evaluate the interaction of reflex gain and noise efficiently. All other parameters were constant at the values listed in Table I.

Fig. 5(d) shows that the %VAF between the simulated noise-free and predicted torques varied with the time. We see that the algorithm estimated all torques accurately until 12 s from the start. This corresponded to the time when the SNR was low; Fig. 6 shows how the %VAF varied with the SNR. The total (blue) and intrinsic torques (green) were predicted well (%VAF $>$ 90%) for SNRs above 5 dB and at all levels of reflex gains. The quality of the reflex identification (red) was also poor at SNRs below 5 dB; however, the %VAF was below 90% at higher SNRs when the reflex gain was low. This drop in the quality of the reflex identification with decreasing reflex gain had little effect on the total %VAF. This is likely because the reflex pathway contributed less to the total output torque at low gains, and consequently, intrinsic torque dominated.

4) Number of Realization: The final simulation series examined the influence of the number of realizations in the ensemble on the quality of the identification. This was done by determining the minimum SNR required to achieve reliable identification for a given number of realizations. The minimum SNR was computed as the SNR at the time at which the model failed to account for any variance.

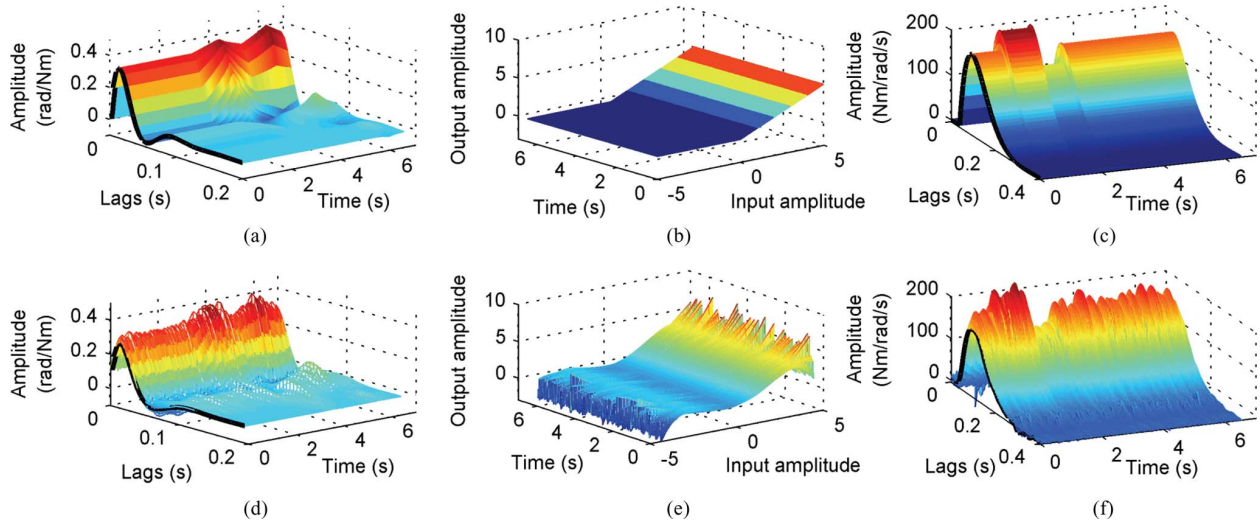

Fig. 2. *Top row*: Simulated intrinsic and reflex stiffness ensembles. (a) Intrinsic compliance IRFs. (b) Static nonlinearities. (c) Reflex stiffness IRFs. *Bottom row*: Estimated intrinsic and reflex stiffness ensembles. (d) Intrinsic compliance IRFs. (e) Static nonlinearities. (f) Reflex stiffness IRFs.

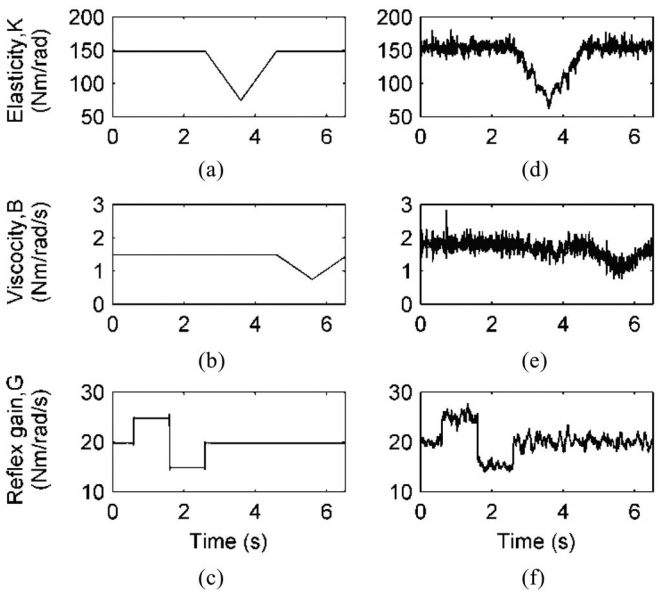

Fig. 3. *Left column*: Time course of simulation parameters: (a) Elasticity, *K*, (b) Viscosity, *B*, (c) Reflex gain, *G*. *Right column*: Parameter values fit to TVPC model estimates: (d) *K*, (e) *B*, and (f) *G*.

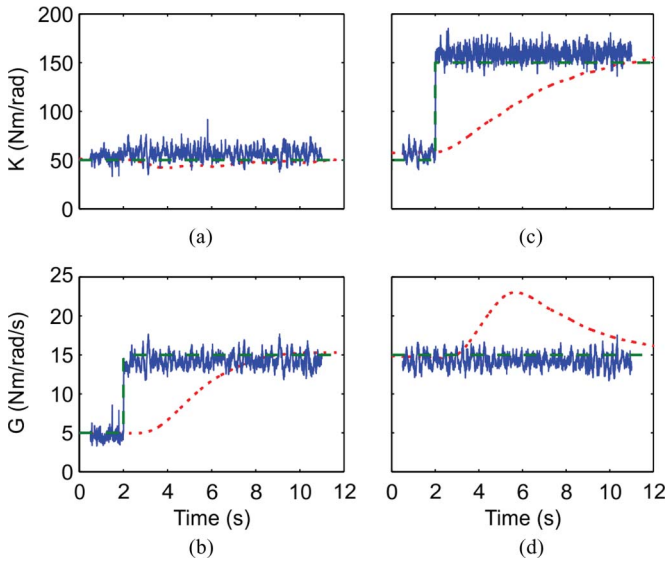

Fig. 4. Comparison between TVPC and adaptive algorithm: (a), (b) Changes in the estimates of *K* and *G* when the value of *G* undergoes a step change at 2 s. (c), (d) Estimates of *K* and *G*, when the value of *K* undergoes a step change at 2 s. The blue solid lines show the estimates generated by the TVPC, the red dotted lines show the estimates from the adaptive algorithm, and the green dashed lines show the simulated values.

Fig. 7 shows that as expected the number of realizations required for reliable identification decreased as the SNR increased. Fewer than 600 realizations were required for a 10-dB SNR and only 200 for a 30-dB SNR.

IV. Discussion

This paper presents a new algorithm that uses ensemble methods for the TV identification of ankle stiffness. Intrinsic and reflex stiffness are iteratively identified using established ensemble methods. The performance limits of the algorithm were explored using simulations. These showed that the TVPC algorithm is capable of identifying rapidly changing system dynamics, even step changes. Furthermore, the algorithm performed well in the presence of noise; the quality of the identification degraded slightly as the SNR decreased. The quality of the system estimates improved by increasing the number of realizations in the data ensembles; more realizations were required as the SNR dropped.

A. Identification of TV Changes

The first simulation series showed that the TVPC algorithm could estimate TV changes in the underlying system parameters. The algorithm successfully estimated both intrinsic and

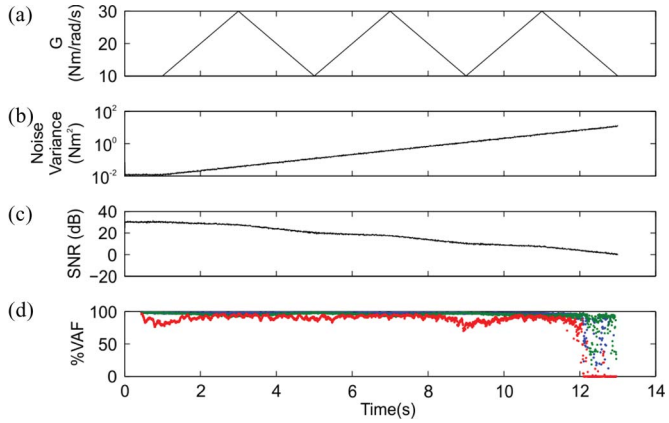

Fig. 5. (a) Reflex gain and (b) noise variance were varied with time, resulting in a varying (c) SNR and (d) %VAF (total: blue; intrinsic: green; reflex: red).

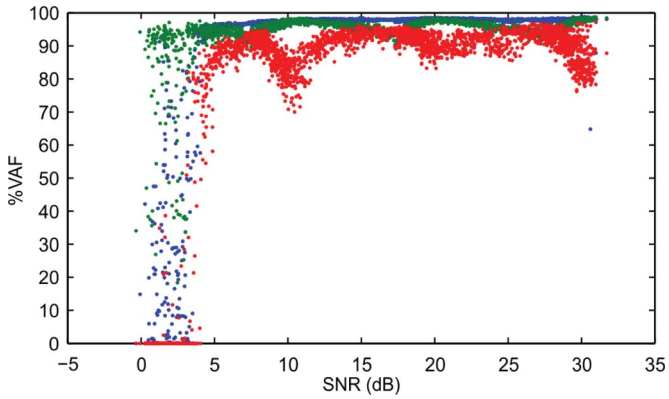

Fig. 6. %VAF of total (blue), intrinsic (green), and reflex (red) torque as functions of the SNR. At SNRs greater than 5 dB, algorithm estimates all three torques quite well with %VAF of over 80%.

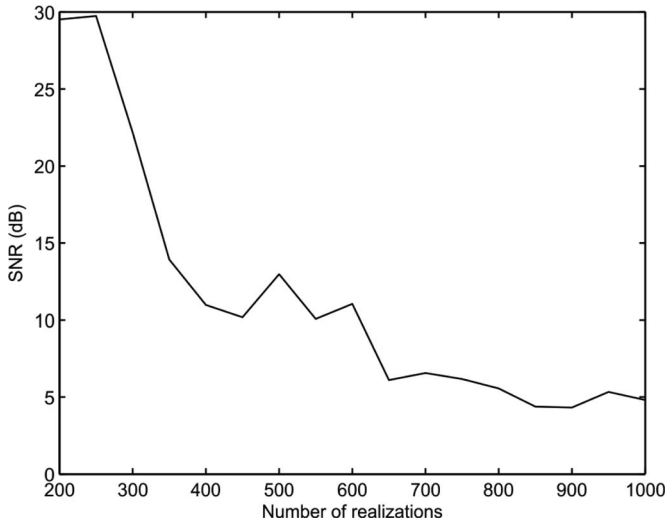

Fig. 7. Minimum SNR required for algorithm to successfully estimate TV joint stiffness for different ensemble sizes.

reflex stiffness during rapid changes with both ramp and step trajectories. In contrast, our previous adaptive algorithm required 10 s to adapt to the change. This sluggish behavior was due to the time needed by the algorithm to perform averaging. All adaptive algorithms require some time to perform the needed averaging and, thus, cannot estimate changes in system behavior as quickly as the TV algorithm can. Furthermore, though not shown, the adaptive algorithm will not respond to quick short-lasting changes in the underlying parameters as those shown in Fig. 3, and thus, these changes are ignored by the adaptive algorithm. This is also due to the averaging of the adaptive algorithm, as a short-lasting change in system parameters will be lost in the averaging performed by the algorithm. Adaptive algorithms are useful for following changes in the state of the system; however, they are inappropriate for measuring how the system changes from state to state or the exact timing of these changes. The TVPC algorithm is well suited for this type of estimation.

B. Performance Limitations

The simulation study showed that the quality of the estimates depended on the relative strength of the parallel pathways. It is not surprising that the quality of the reflex identification degrades as the gain drops, because of the iterative nature of the identification procedure. Recall that intrinsic stiffness is identified first and its contribution to the output torque is removed prior to the reflex identification. However, all the noise remains during the reflex identification. Therefore, for a given overall SNR, the reflex identification sees relatively more noise as the reflex gain drops. Conversely, if the reflex pathway dominated the output, the intrinsic identification would be expected to yield poorer results for similar reasons. However, even for matched effective SNRs, it is likely that the quality of the reflex identification will be lower. Reflex stiffness presents a more difficult estimation problem, since there are many more unknown parameters to identify, (i.e., the reflex IRF is longer than the intrinsic stiffness IRF and the reflex nonlinearity must also be identified).

The relative gain of the pathways cannot be controlled experimentally. Therefore, to improve estimates, the size of the data ensemble must be increased. This study showed that increasing the number of realizations in the data ensembles improved the quality of the estimates in the presence of noise. This would impact most significantly the identification of the pathway most sensitive to noise, in this case, the reflex identification. Fig. 7 shows that relatively few realizations were required for reliable identification; however, increasing the size of the ensemble would improve the estimates. Therefore, when planning an experiment, the minimum number of realizations for reliable identification must be used, but for better estimates, it would be advisable to include more realizations.

Stationary studies have typically found an SNR of about 10 dB [6]. For such conditions, the number of realizations necessary for good results would be between 600 and 800. A typical realization of a rapid movement takes 3 s to complete; therefore, 800 realizations would take 40 min plus rest periods to complete; this is not an unreasonable length for an experiment. Thus, the amount of data needed for the TV algorithm does not create unreasonable demands on human subjects, and can be used to measure TV joint stiffness experimentally.

C. Applications of the TV Algorithm

Previous studies identified ankle stiffness for a particular operating point and showed that stiffness was a nonlinear function of position and background torque levels [6]. These results emphasize the highly nonlinear nature of this physiological system. Ideally, a global model would be developed that would incorporate all the underlying nonlinearities, and so be capable of predicting ankle stiffness throughout any task. Unfortunately, this is not yet possible.

Varying joint position or torque with time causes the parameters of the PC model to change. Even though these changes are not explicitly dependent on time, but rather depend on unmodeled nonlinear behavior, treating them as TV parameters allows them to be modeled in a task-specific manner. The TVPC algorithm can be used to study how the PC model changes throughout a particular task due to the nonlinearities. The identified system will not be able to predict the stiffness modulation pattern during a different task but can define the role it plays in specific situations without requiring a global model.

Knowledge of how intrinsic and reflex stiffness change during movement is essential to understanding the central control mechanisms. Thus, knowledge of the exact timing of stiffness changes during movement would help to answer the on-going debate between equilibrium point control hypothesis and the internal models hypothesis. The equilibrium point hypothesis postulates that the CNS controls the position of joint by controlling the joint stiffness. In this model, movement is accomplished by altering the spring-like properties of muscle and by changing the feedback generated by the reflex stiffness [27]–[29]. The internal model hypothesis posits that the CNS has an internal model of the dynamics of the limb and the load, and predicts the exact forces needed to generate the movement [29], [30]. By determining whether the changes in stiffness associated with movement precede or succeed the movement, it may be possible to solve the debate.

Another area of research that may be aided by this algorithm is the design of prostheses. When designing a biomimetic prosthesis, it is preferable if the stiffness of the prosthesis is similar to that of the joint [31]. The TVPC algorithm can estimate stiffness during movement, and thus allow for construction of prosthesis that better model the joint they are replacing.

We conclude that the TVPC algorithm will be a useful tool in the study of joint stiffness during nonstationary tasks and that it will help further the understanding of the nonlinear nature of this complex physiological system.

ACKNOWLEDGMENT

The authors would like to acknowledge the contributions made by M. Baker in the development of the algorithm.

REFERENCES

[1] R. E. Kearney and I. W. Hunter, "System identification of human joint dynamics," *Crit. Rev. Biomed. Eng.*, vol. 18, pp. 55–87, 1990.

[2] J. D. Brooke, J. Cheng, D. F. Collins, W. E. McIlroy, J. E. Misiaszek, and W. R. Staines, "Sensori-sensory afferent conditioning with leg movement: Gain control in spinal reflex and ascending paths," *Progr. Neurobiol.*, vol. 51, pp. 393–421, Mar. 1997.

[3] J. D. Brooke, W. E. Mcilroy, D. F. Collins, and J. E. Misiaszek, "Mechanisms within the human spinal-cord suppress fast reflexes to control the movement of the legs," *Brain Res.*, vol. 679, pp. 255–260, May 15, 1995.

[4] C. Capaday and R. B. Stein, "Difference in the amplitude of the human soleus h reflex during walking and running," *J. Physiol.-Lond.*, vol. 392, pp. 513–522, Nov. 1987.

[5] T. Kimura, D. Nozaki, K. Nakazawa, M. Akai, and T. Ohtsuki, "Gradual increment/decrement of isometric force modulates soleus stretch reflex response in humans," *Neurosci. Lett.*, vol. 347, pp. 25–28, Aug. 14, 2003.

[6] M. M. Mirbagheri, H. Barbeau, and R. E. Kearney, "Intrinsic and reflex contributions to human ankle stiffness: Variation with activation level and position," *Exp. Brain Res.*, vol. 135, pp. 423–436, Dec. 2000.

[7] R. E. Kearney, M. Lortie, and R. B. Stein, "Modulation of stretch reflexes during imposed walking movements of the human ankle," *J. Neurophysiol.*, vol. 81, pp. 2893–2902, Jun. 1999.

[8] T. Sinkjaer, J. B. Andersen, and B. Larsen, "Soleus stretch reflex modulation during gait in humans," *J. Neurophysiol.*, vol. 76, pp. 1112–1120, Aug. 1996.

[9] E. P. Zehr and R. B. Stein, "What functions do reflexes serve during human locomotion?" *Progress Neurobiol.*, vol. 58, pp. 185–205, Jun. 1999.

[10] R. B. Stein and R. E. Kearney, "Nonlinear behavior of muscle reflexes at the human ankle joint," *J. Neurophysiol.*, vol. 73, pp. 65–72, Jan. 1995.

[11] J. B. Andersen, B. Larsen, and T. Sinkjaer, "Modulation of the human soleus stretch reflex during gait," presented at the 16th Annu. Int. Conf. of the IEEE Engineering in Medicine and Biology Society, Denmark, 1994.

[12] J. B. Andersen and T. Sinkjaer, "Afferent input from the human ankle extensors during walking," presented at the 20th Annu. Int. Conf. of the IEEE Engineering in Medicine and Biology Society, Hong Kong, 1998.

[13] R. F. Kirsch and R. E. Kearney, "Identification of time-varying dynamics of the human triceps surae stretch reflex.2. rapid imposed movement," *Exp. Brain Res.*, vol. 97, pp. 128–138, Dec. 1993.

[14] R. E. Kearney, R. B. Stein, and L. Parameswaran, "Identification of intrinsic and reflex contributions to human ankle stiffness dynamics," *IEEE Trans. Biomed. Eng.*, vol. 44, no. 6, pp. 493–504, Jun. 1997.

[15] L. Galiana, J. Fung, and R. Kearney, "Identification of intrinsic and reflex ankle stiffness components in stroke patients," *Exp. Brain Res.*, vol. 165, pp. 422–434, Sep. 2005.

[16] M. M. Mirbagheri, H. Barbeau, M. Ladouceur, and R. E. Kearney, "Intrinsic and reflex stiffness in normal and spastic, spinal cord injured subjects," *Exp. Brain Res.*, vol. 141, pp. 446–459, Dec. 2001.

[17] D. Ludvig and R. E. Kearney, "Real-time estimation of intrinsic and reflex stiffness," *IEEE Trans. Biomed. Eng.*, vol. 54, no. 10, pp. 1875–1884, Oct. 2007.

[18] M. Lortie and R. E. Kearney, "Identification of physiological systems: Estimation of linear time-varying dynamics with nonwhite inputs and noisy outputs," *Med. Biol. Eng. Comput.*, vol. 39, pp. 381–390, May 2001.

[19] M. Lortie and R. E. Kearney, "Identification of time-varying Hammerstein systems from ensemble data," *Ann. Biomed. Eng.*, vol. 29, pp. 619–635, 2001.

[20] M. Baker, Y. Zhao, D. Ludvig, R. Wagner, and R. Kearney, "Time-varying parallel-cascade system identification of ankle stiffness from ensemble data," in *Proc. 26th Annu. Int. Conf. IEEE Eng. Medicine and Biology Society (EMBS)*, San Francisco, CA, 2004, pp. 4688–4691.

[21] H. I. Giesbrecht, M. Baker, D. Ludvig, R. Wagner, and R. E. Kearney, "Identification of time-varying intrinsic and reflex joint stiffness," in *Proc. 28th Annu. Int. Conf. IEEE Eng. Medicine and Biology Society (EMBS)*, New York, 2006, pp. 288–291.

[22] T. Starret Visser, D. Ludvig, and R. E. Kearney, "Performance evaluation of an algorithm for the time-varying identification of ankle stiffness," in *Proc. 31st Annu. Int. Conf. IEEE Eng. Medicine and Biology Society (EMBS)*, Minneapolis, MN, 2009, pp. 3995–3998.

[23] R. E. Kearney and I. W. Hunter, "Nonlinear identification of stretch reflex dynamics," *Ann. Biomed. Eng.*, vol. 16, pp. 79–94, 1988.

[24] P. L. Weiss, R. E. Kearney, and I. W. Hunter, "Position dependence of ankle joint dynamics—Part I: Passive mechanics," *J. Biomech.*, vol. 19, pp. 727–735, 1986.

[25] P. L. Weiss, I. W. Hunter, and R. E. Kearney, "Human ankle joint stiffness over the full range of muscle activation levels," *J. Biomech.*, vol. 21, pp. 539–544, 1988.

[26] D. W. Marquardt, "An algorithm for the least-squares estimation of nonlinear parameters," *J. Soc. Ind. App. Math.*, vol. 11, pp. 431–441, 1963.

[27] S. V. Adamovich, M. F. Levin, and A. G. Feldman, "Central modifications of reflex parameters may underlie the fastest arm movements," *J. Neurophysiol.*, vol. 77, pp. 1460–1469, Mar. 2011.
[28] H. Gomi and M. Kawato, "Human arm stiffness and equilibrium-point trajectory during multi-joint movement," *Biol. Cybern.*, vol. 76, pp. 163–171, Mar. 1997.
[29] D. M. Wolpert and Z. Ghahramani, "Computational principles of movement neuroscience," *Nat. Neurosci.*, vol. 3 Suppl, pp. 1212–1217, Nov. 2000.
[30] M. Kawato, "Internal models for motor control and trajectory planning," *Curr. Opin. Neurobiol.*, vol. 9, pp. 718–727, Dec. 1999.
[31] A. H. Hansen, D. S. Childress, S. C. Miff, S. A. Gard, and K. P. Mesplay, "The human ankle during walking: implications for design of biomimetic ankle prostheses," *J. Biomech.*, vol. 37, pp. 1467–1474, Oct. 2004.

Daniel Ludvig (S'06–M'11) received the B.Sc. degree in physiology and physics in 2003, the M.Eng. degree in biomedical engineering in 2006, and the Ph.D. degree in biomedical engineering in 2010, all from McGill University, Montreal, QC, Canada.

He is currently a Postdoctoral Fellow in the Sensory Motor Performance Program at the Rehabilitation Institute of Chicago, Chicago, IL. His research interests include the use of systems identification in investigating human motor control systems. In particular, his research involves modeling how humans maintain posture and control movements of their limbs.

Dr. Ludvig is a member of the Society for Neuroscience and the Society for the Neural Control of Movement.

Tanya Starret Visser received the B.Eng. degree in electrical and biomedical engineering in 2007 from McMaster University, Hamilton, ON, Canada and the M. Eng. degree in biomedical engineering in 2009 from McGill University, Montreal, QC, Canada.

Heidi Giesbrecht received the B.Eng. degree in mechanical engineering in 2004, and the M.Eng. degree in biomedical engineering in 2007, both from McGill University, Montreal, QC, Canada.

Robert E. Kearney (M'76–SM'92–F'01) received the Ph.D. degree in mechanical engineering from McGill University, Montreal, QC, Canada, in 1976.

He is a Professor in the Department of Biomedical Engineering, Faculty of Medicine, McGill University. He maintains an active research program that focuses on using quantitative engineering techniques to address biomedical research problems. His research interests include the development of algorithms and tools for biomedical system identification; the application of system identification to understand the role played by stretch reflexes and joint mechanics in the control of posture and movement; and the development of bioinformatics tools and techniques for proteomics.

Dr. Kearney is a Fellow of the Engineering Institute of Canada, the American Institute of Medical and Biological Engineering, and a recipient of the IEEE Millennium medal.